A founder mutation in EHD1 presents with tubular proteinuria and deafness

Running title: Proteinuria, deafness and EHD1

Naomi Issler [1#], Sara Afonso [2#], Irith Weissman [3#], Katrin Jordan [2], Alberto Cebrian-Serrano [4], Katrin Meindl [2], Eileen Dahlke [5], Konstantin Tziridis [6], Guanhua Yan [7], José M. Robles-López [7], Lydia Tabernero [7], Vaksha Patel [1], Anne Kesselheim [1], Enriko D. Klootwijk [1], Horia C. Stanescu [1], Simona Dumitriu [1], Daniela Iancu [1], Mehmet Tekman [1], Monika Mozere [1], Graciana Jaureguiberry [1], Priya Outtandy [1], Claire Russell [7], Anna-Lena Forst [2], Christina Sterner [2], Elena-Sofia Heinl [2], Helga Othmen [2], Ines Tegtmeier [2], Markus Reichold [2], Ina Maria Schiessl [9], Katharina Limm [10], Peter Oefner [10], Ralph Witzgall [11], Lifei Fu [12], Franziska Theilig [5], Achim Schilling [6], Efrat Shuster Biton [3], Limor Kalfon [3], Ayalla Fedida [3], Elite Arnon-Sheleg [3], Ofer Ben Izhak [13], Daniella Magen [13], Yair Anikster [14], Holger Schulze [6], Christine Ziegler [12], Martin Lowe [7], Benjamin Davies [4], Detlef Böckenhauer [1], Robert Kleta [1*#], Tzipora C. Falik Zaccai [3#], Richard Warth [2*#]

# contributed equally

[1] Department of Renal Medicine, UCL, London, UK
[2] Medical Cell Biology, University Regensburg, Germany
[3] Galilee Medical Center, Nahariya, Israel
[4] Wellcome Centre Human Genetics, University Oxford, UK
[5] Institute of Anatomy, University Kiel, Germany
[6] ENT Clinic, University Hospital Erlangen, Germany
[7] Division of Molecular & Cellular Function, University Manchester, UK
[8] Royal Veterinary College, London, UK
[9] Institute of Physiology, University Regensburg, Germany
[10] Institute of Functional Genomics, University Regensburg, Germany
[11] Molecular and Cellular Anatomy, University Regensburg, Germany
[12] Structural Biology, University Regensburg, Germany
[13] Pediatric Nephrology Institute, Haifa, Israel
[14] Sheba Medical Center, Tel-Aviv, Israel

*Corresponding authors:

Robert Kleta, MD/PhD
Potter Chair of Nephrology
Department of Renal Medicine
University College London
Rowland Hill Street, London NW3 2PF, UK
phone: ++44-20 7314 7554
email: r.kleta@ucl.ac.uk

Richard Warth, MD
Medical Cell Biology
University Regensburg
Universitaetsstr. 31, 93053 Regensburg, Germany
phone: ++49 941 943 2894
email: richard.warth@ur.de

Key words:
Epithelial transport physiology, Infertility, Megalin, Eps15 Homology Domain, proximal tubule, genetic renal disease

Significance Statement

Renal tubular protein reabsorption has been the focus of interest in the kidney community, and despite numerous associated inherited diseases, the detailed molecular basis remains poorly understood. Based on six patients with tubular proteinuria and sensorineural hearing deficit, EHD1 was identified as a critical component of the renal protein reabsorption machinery and inner ear function. As a key player in vesicular dynamics, EHD1 has previously been associated with early ciliogenesis. However, no obvious defect of ciliogenesis was found in the kidney of either the patients studied here or in knockin and knockout mice. In summary, these data may contribute to a better understanding of the functional relevance of EHD1 in human tissues, particularly in the kidney and inner ear.

Abstract

Background: The endocytic reabsorption of proteins in the proximal tubule requires a complex machinery and defects can lead to tubular proteinuria. The precise mechanisms of endocytosis and processing of receptors and cargo are incompletely understood. EHD1 belongs to a family of proteins presumably involved in the scission of intracellular vesicles and in ciliogenesis. However, the relevance of EHD1 in human tissues, in particular the kidney, was unknown.

Methods: Genetic techniques were used in patients with tubular proteinuria and deafness to identify the disease-causing gene. Diagnostic and functional studies were performed in patients and disease models to investigate the pathophysiology.

Results: We identified six individuals (5-33 years) with proteinuria and a high-frequency hearing deficit associated with the homozygous missense variant c.1192C>T (p.R398W) in *EHD1*. Proteinuria (0.7-2.1 g/d) consisted predominantly of low-molecular-weight proteins, reflecting impaired renal proximal tubular endocytosis of filtered proteins. *Ehd1* knockout and *Ehd1*$^{R398W/R398W}$ knockin mice also showed a high-frequency hearing deficit and impaired receptor-mediated endocytosis in proximal tubules, and a zebrafish model showed impaired ability to reabsorb low-molecular-weight dextran. Interestingly, ciliogenesis appeared unaffected in patients and mouse models. *In silico* structural analysis predicted a destabilizing effect of the R398W variant and possible inference with nucleotide-binding leading to impaired EHD1 oligomerization and membrane remodeling ability.

Conclusion: A previously unrecognized autosomal recessive disorder characterized by sensorineural deafness and tubular proteinuria is caused by a homozygous missense variant in *EHD1*. Recessive *EHD1* variants should be considered in individuals with hearing impairment, especially if tubular proteinuria is noted.

Introduction

Endocytosis refers to the mechanism by which cells internalize macromolecules and particles into transport vesicles derived from the plasma membrane [1]. It is a crucial and regulated pathway for entry into the cell involved in numerous processes, including neurotransmission, signal transduction, immune response and cellular homeostasis. In the kidney, endocytosis is critical for the reabsorption of filtered macromolecules, such as LMW proteins. Investigations of rare diseases associated with LMW proteinuria have identified important roles for several cellular proteins involved in this process. Most filtered macromolecules are retrieved from the proximal tubular lumen by the promiscuous receptors Megalin, Cubilin and Amnionless [2], Mutations in the encoding genes *LRP2*, *CUBN* and *AMN* cause Donnai-Barrow syndrome (MIM222448) and Imerslund-Grasbeck syndrome (MIM261100 and 618882), respectively [3-5]. Following endocytosis and release of cargo in the endosome, the receptors are recycled to the plasma membrane, while the cargo is transported to its downstream destination, either the lysosome (degradation) or the basolateral membrane (transepithelial transport) [2]. An important regulator of this sorting process is the phosphatidylinositol 5'-phosphatase OCRL, mutations in which cause Lowe syndrome (MIM309000), whereas the chloride/proton antiporter CLCN5 is involved in endosomal acidification and constitutes the molecular basis of Dent disease (MIM300009); both clinically showing LMW proteinuria [6].

Here we report on our investigations related to patients who presented with LMW proteinuria and sensorineural deafness with neither pathogenic variants in known disease genes nor other defining phenotypes associated with these known disorders. Instead, genetic analysis revealed a homozygous missense mutation in the EHD1 gene.

EHD1 is one of four mammalian dynamin-like C-terminal Eps15 Homology Domain (EHD) proteins and localized to several cytoplasmic vesicular structures, including endocytic vesicles and the Golgi apparatus [7]. The EHD proteins have been previously implicated in endosomal scission, so that receptor

and cargo can be separated in order to be processed to their respective proper destinations [8, 9]. Yet, studies in knockout mice have yielded variable results, ranging from a subclinical phenotype to abnormal sperm development to eye abnormalities to impaired ciliogenesis to embryonic lethality [10-14]. Interestingly, none of these studies found a role for EHD1 in the kidney or inner ear.

Methods

Full details of all methods can be found in the Supplement.

Ethics

The study was performed in accordance with the Declaration of Helsinki. It was approved by by the IRB of the Galilee Medical Center in Naharia (study # 06022007), and by the supreme Helsinki committee of the Israeli Ministry of Health (study # 920070611). The first patient was recruited on May 1st 2008, the last patient was recruited on July 11th 2018. Informed consent was obtained directly from the adult participant and from the parents of participants aged 18 years and younger. All clinical examinations and investigations were performed at the discretion of the treating clinician as part of the patients' diagnosis and treatment.

Genetic studies

Genotyping, linkage studies and whole exome sequencing were performed as described previously [15]. Variants were assessed using a custom-built in-house software pipeline [16], as well as the Ingenuity platform (https://variants.ingenuity.com/qci/).

Animal models

Experiments were performed according to the guidelines for the care and use of laboratory animals published by the US National Institutes of Health and were approved by the local councils for animal care. *Ehd1* knockout mice were generated by the Sanger Institute, as described previously [17] and acquired from the European Mouse Mutant Archive (MGI ID: 4432418). *Ehd1* knockin mice were generated at the Wellcome Trust Centre for Human Genetics, University of Oxford, United Kingdom. Animal experiments on mice to assess renal function were approved by the "Regierung Unterfranken",

Germany. Zebrafish were studied for renal tubular LMW dextran handling as described previously [18]. For details please see the Supplement.

Renal elimination of labelled β_2-microglobulin

A recombinant human β_2-microglobulin expressed in *E. coli* (Merck, #475828) was conjugated with the fluorescent tag Alexa Fluor™ 546 and injected into anesthetized mice. After 30 min, urine and blood were collected and tissue fixation was performed. The fluorescence of β_2-microglobulin-Alexa Fluor 546 in urine, serum and kidney lysate samples was measured.

Intravital imaging of proximal tubular protein reabsorption

Mice were anesthetized and the left kidney was exposed. To label the vasculature, a 25 mg/ml solution of FITC-500 kDa Dextran conjugate was used. After 1 min β_2-microglobulin-Alexa Fluor 546 was injected intravenously and the proximal tubular uptake was measured as increase in tubular fluorescence intensity (up to 30 min after injection).

Auditory brainstem response measurements

Anesthetized mice aged 6-9 weeks were used for the measurement of the auditory brainstem response. Stimuli presented were pure tones at 4, 8, 16 and 32 kHz.

Statistics

Data are shown as mean values ± standard error of the mean (SEM); "n" stands for the number of observations. Two-sided unpaired Student's t-test and ANOVA were used to calculate significance between different groups as appropriate. A p-value ≤ 0.05 was accepted to indicate statistical significance.

Results

Patients

We identified six individuals from four families with an unexplained unique phenotype of LMW proteinuria and sensorineural hearing loss. Proteinuria was discovered incidentally by dipstick (trace to 2+) during investigations for minor illnesses. Four individuals had kidney biopsies performed due to proteinuria, which all were reported as being normal (Figure 1). Renal ultrasound studies showed normal findings. Proteinuria was noted to contain highly elevated levels of LMW protein, including β_2-microglobulin and retinol binding protein, consistent with a defect in proximal tubular protein re-uptake (Figure 1 and Supplemental Table 1).

One individual had a DMSA scan because of suspected urinary tract infection which surprisingly showed globally impaired uptake of the tracer by the kidneys (Figure 1). Subsequently, other affected individuals also underwent DMSA scans with similarly impaired uptake.

The hearing problem was identified during the clinical work-up for this disorder. Audiograms in affected individuals revealed high-frequency hearing loss, consistent with sensorineural hearing impairment (Figure 1).

All affected individuals underwent detailed clinical examinations including formal neurological and ophthalmological assessments and no other abnormalities were identified. No dysmorphologies were noted. Blood studies for renal glomerular function including Vitamin B12 showed no abnormalities. One individual became pregnant and delivered a healthy child. No affected male has so far had progeny. All individuals belong to a Druze ethnic-religious group in Palestine (pedigrees Figure 2).

Genetic studies

Linkage analysis identified a single significant region of interest comprising approximately 1.5 million bases on chromosome 11, with a significant LOD score of 7.2 (Figure 2). This small 1.5 cM locus was defined by two flanking SNPs: rs7131675 and rs2845570. Exome sequencing revealed in the linked

interval a single homozygous variant that segregated with the phenotype, located in *EHD1*: c.1192C>T; p.(R398W). The damage prediction algorithms indicated functional impairment: CADD score: 32 (likely deleterious); SIFT: 0.01 (deleterious); Polyphen: 0.677 (possibly damaging). This variant is also annotated as rs151119199 in dbSNP (https://www.ncbi.nlm.nih.gov/snp/) and has an allele frequency of 0.00001427 in the gnomAD database (https://gnomad.broadinstitute.org, accessed June 2021). Sequencing of genetically matched healthy Druze identified this variant in one of 196 alleles indicating a strongly increased allele frequency in this population.

EHD1 and kidney

In human kidney, we identified EHD1 predominantly in the subapical compartment of proximal tubular epithelial cells (Figure 3 and Supplemental Figure 1). This was confirmed in mouse kidney, where Ehd1 partially co-localized with the endocytic tracer β_2-microglobulin and the apical receptor proteins Megalin and Cubilin (Figure 4 and Supplemental Figures 2 and 3). Interestingly, localization and abundance of Megalin and Cubulin appeared unaffected by Ehd1 knockout and knockin (Figure 4 and Supplemental Figure 6). *Ehd1* knockout and antibody specificity were confirmed by the presence or absence of Ehd1 staining in wildtype and *Ehd1*$^{-/-}$ mice, respectively (Supplemental Figure 2).

For functional assessment we first assessed *ehd1* in zebrafish. There are two orthologues in zebrafish *ehd1a* and *ehda1b,* both of which are expressed in kidney. When suppressing both paralogues with morpholinos, morphant zebrafish larvae had a significantly impaired ability to reabsorb low-molecular weight dextran compared to control larvae (Supplemental Figure 4).

For a more detailed assessment, we investigated *Ehd1* knockout mice (*Ehd1*$^{-/-}$). We first measured LMW protein uptake using fluorescently labelled β_2-microglobulin. This showed a substantial decrease in re-uptake in *Ehd1*$^{-/-}$ versus wildtype mice resulting in increased urinary excretion (Figure 3). For better assessment of the R398W variant identified in our patients, we also generated R398W knockin mice (*Ehd1*$^{R398W/R398W}$). Mutant Ehd1 protein appeared to have largely decreased expression in

proximal tubules and was predominantly localized in small intracellular aggregates (Figure 4, Supplemental Figure 5). In distal nephron segments, mutant Ehd1 was also present in elongated structures that were negative for acetylated tubulin, a marker for cilia (Supplemental Figure 5). These elongated apical structures were not found in wildtype kidneys. In order to gain more mechanistic insights, a possible effect of Ehd1 inactivation on Arf6 and Rab11, two factors involved in trafficking of membranes, was examined. Interestingly, localization and abundance of Arf6 and Rab11 appeared normal in proximal tubules of knockout and knockin mice (Supplemental Figures 6 and 7). Consistent with our patients and *Ehd1*$^{-/-}$ mice, *Ehd1*$^{R398W/R398W}$ mice had increased levels of fluorescent β_2-microglobulin in the urine (Figure 3). Moreover, whereas in wildtype mice reabsorbed fluorescent β_2-microglobulin was mainly confined to the early segments of proximal tubule, in the genetically modified mice it was present throughout the proximal tubule, consistent with compensatory uptake in later segments of the proximal tubule (Figure 3). Similarly, *in vivo* imaging of mouse kidneys using multiphoton microscopy showed a significantly lower β_2-microglobulin uptake rate in *Ehd1*$^{-/-}$ mice (Figure 3 and Supplemental Figure 8).

EHD1 and inner ear

Because of the sensorineural deafness of our patients, we investigated expression of Ehd1 in mouse inner ear and identified strong expression in the stria vascularis (Figure 5). Knockout and knockin mice had a loss and altered pattern of Ehd1 expression, respectively (Figure 5). Importantly, *Ehd1*$^{R398W/R398W}$ mice also displayed a significant high-frequency hearing impairment of 20-30 dB compared to age-matched wildtype mice (Figure 5).

Cellular studies

We further investigated the cellular consequences of the R398W mutant EHD1 in a proximal tubular cell line, LLC-PK1, genetically modified to either express wildtype or mutant EHD1 when induced with

tetracycline. Cells with wildtype EHD1 showed a spotted distribution pattern as described [19]. In contrast, mutated EHD1 expressing cells showed elongated tubular structures, presumably tubular recycling endosomes, indicating an impairment of membrane fission events (Figure 6). EHD1 is a component of a complex multi-protein membrane shaping machinery. Previous work has indicated that EHD1 together with other proteins, e.g. Pacsin 2, MICAL-L1, and ARF6, functions in endosomal recycling [19-21]. Therefore, we investigated the effect of the EHD1^{R398W} mutation on the distribution of MICAL-L1 and Pacsin 2. Interestingly, MICAL-L1 remained associated to EHD1 in cells overexpression mutant EHD1 and similarly Pacsin 2. These data indicate that the elongated structures observed in cells with mutant EHD1^{R398W} are in fact abnormal tubular recycling endosomes (Supplemental Figures 9 and 10).

We also investigated protein stability. After removal of tetracycline, levels of both wildtype and mutant EHD1 were similar, but levels of mutant EHD1 reduced significantly faster, consistent with impaired protein stability of mutant EHD1 (Figure 6). This finding is in agreement with the reduced protein abundance observed in kidneys of *Ehd1* knockin mice (Supplemental Figures 2 and 5).

Role of Ehd1 in renal ciliogenesis

Due to the previously reported role of EHD1 in cilia formation, we assessed cilia morphology [14, 22, 23]. Interestingly, primary cilia were present and appeared to have normal morphology within the proximal tubule in affected individuals, knockout as well as knockin animals (Supplemental Figure 11) [24].

In silico structural modelling

Structural analysis identified the mutated EHD1 R398 as part of the α-helix 12, presumably involved in oligomerization of EHD1 (Figure 7 and Supplemental Figures 12-14). Replacement of arginine with tryptophan at this position is predicted to disrupt the stability of interactions between EHD1 dimers

leading to mechanically instable oligomerization and the inability to process membrane scission. Another consequence of the R398W mutation is its possible inference with the nucleotide-binding pocket of an adjacent EHD1 (Figure 7).

Discussion

Our work describes a previously unrecognized syndrome presenting with LMW proteinuria and sensorineural deafness. An isolated population provided us with the opportunity to investigate this *EHD1* related syndrome. The unambiguous identification of an identical homozygous genetic variant in four families from the same ethnic background strongly suggests the presence of a founder mutation, consistent with the apparent increased allele frequency of this *EHD1* missense variant in the Druze population.

Our clinical, genetic and molecular findings are fully compatible with partial or organ specific loss of EHD1 function as disease mechanism, consistent with autosomal recessive inheritance. The gnomAD database shows that *EHD1* is highly constrained and that predicted loss of function variants are significantly less observed than expected (probability of loss of function intolerance = 0.98) suggesting that this ubiquitously expressed protein has a unique and critical biological function [25, 26]. Arguably, complete loss of function may not be compatible with human life and the R398W variant potentially retains some functionality or heterozygous loss of function entails a reproductive disadvantage [26].

We provide compelling experimental evidence for the role of EHD1 in biology by unequivocally linking it to a distinct human phenotype, i.e. to disease mechanisms related to renal proximal tubular endocytosis and sensorineural deafness. We demonstrate EDH1 related kidney phenotypes in man, in zebrafish as well as in knockout and knockin mice. Impaired renal handling of LMW molecules is seen in our patients, in zebrafish as well as in mice with Ehd1 dysfunction. Remarkably, the renal phenotype was milder in mice than in humans, and decreased absorptive capacity was evident only by administration of labeled β_2-microglobulin. Furthermore, we provide evidence for EDH1 related hearing deficits in man and mouse and we speculate that EHD1 dysfunction may interfere with male

fertility based on corroborating data from Ehd1 knockout and additional data from knockin mice (Supplemental Table 2).

Our work identifies EHD1 as a critical component in the endocytic machinery of the renal proximal tubule, aligned with previous work which established a role for EHD1 in endocytic scission and recycling [9]. We noted elongated pathological tubular structures in LLC-PK1 cells expressing mutant EHD1 providing yet another piece of circumstantial evidence for EHD1's role in membrane shaping and fission (Figure 5). In the proximal tubule such scission divides and separates recycling tubules from sorting endosomes, so that receptor proteins handling cargo proteins, such as Megalin can be recycled back to the apical membrane, whereas the cargo proteins can be directed to their respective targets [27]. We propose that these EHD1 related mechanisms explain the reduced capacity of proximal tubular endocytosis and subsequent "overflow" of LMW proteins into the urine. Results from our study are fully consistent with this particular role for EHD1 (Figure 7). Interestingly, localization and abundance of Megalin, Cubilin, Arf6 and Rab11 appeared unaffected in *Ehd1* knockout and knockin mice (Figure 4 and Supplemental Figures 6 and 7). These data suggest that Ehd1 does not physically bind to these proteins, but that its inactivation or mutation slows down vesicle fission and thus transport rates.

Our data and damage prediction algorithms, such as a CADD score of 32, indicated functional impairment of the p.R398W mutant. A closer look into publicly available structure biology databases revealed how the identified missense mutation p.R398W may impair EHD1 function. On the molecular level, *in silico* modelling suggested that the mutation hinders the formation of EHD1 oligomers necessary for association with endosomes and membrane scission (Figure 7) [28-30]. Thus, structural modeling supported a direct effect on scission and as consequence impaired processing of membranes, receptors and cargo. Moreover, the identified *EHD1* mutation can also interfere with the nucleotide-binding site of an adjacent EHD1 (Figure 7). This particular mechanism was further

supported by the extensive tubulation observed in renal proximal tubular cells expressing mutant EHD1 (Figure 6), which in fact is reminiscent of the cellular phenotype of ATPase-deficient mutant T94A in Ehd2 [31]. However, our data do not allow to specify the extent of loss of function for the disease causing R398W variant, yet, the similarity in the phenotypes of *Ehd1*$^{-/-}$ and *Ehd1*$^{R398W/R398W}$ mice strongly suggests that it indeed significantly impairs organ specific functions.

A search of the Shared Harvard Inner-Ear Laboratory Database (SHIELD) revealed that Ehd1 is known to be expressed in the mouse inner ear [32]. The association of EHD1 dysfunction with sensorineural deafness and its expression in stria vascularis (Figure 5) highlights the important role of receptor-mediated endocytosis in inner ear function, consistent with the deafness seen in Donnai-Barrow syndrome, due to mutations in Megalin [3]. While the exact role of Megalin in inner ear function is still unclear, it has been implicated in endocytosis in the endolymphatic sac with prominent expression in vestibular dark cells as well as stria vascularis [33, 34].

Male Ehd1 knockout mice have previously been shown to be infertile [10]. Our results corroborate this and, importantly, male *Ehd1*$^{R398W/R398W}$ mice are also infertile (Supplemental Table 2). However, if this also applies to humans remains to be seen as the young ages of our male patients do not allow any conclusions.

Of further interest is our finding of morphologically normal primary cilia in both patients and genetically modified mice (Supplemental Figure 11) as this is in contrast to previous reports of defects in ciliogenesis in zebrafish and *Ehd1* knockout mice [14, 22, 23]. Ciliopathies typically present in the kidney with cysts, which were not seen in this study. Our findings argue against an essential role of EHD1 in ciliogenesis, at least in the kidney. Of note, defects in ciliogenesis in mice appeared to be dependent on the genetic background of mice [13, 14].

In summary, a previously unrecognized syndrome, characterized by LMW proteinuria and sensorineural deafness accompanied by markedly reduced DMSA uptake in renal imaging, is caused by mutated *EHD1*. Our findings enable an accurate diagnosis, genetic testing and counselling for affected individuals and families. Our findings are consistent with a role for EHD1 as an intracellular membrane-shaping protein involved in vesicular trafficking and recycling. Our work also establishes *EHD1* as a new deafness disease gene. Because of the subtlety of the kidney phenotype, which may go unrecognized in clinical practice, *EHD1* variants should be considered in patients with apparent isolated deafness. Moreover, our study suggests a possible role for *EHD1* in male infertility, thereby corroborating a previous study [10].

The identification of mutated EHD1 being causative for a rare disease entity in an isolated population with its well-defined phenotypes provides solid evidence for EHD1's real role in life. These insights position EHD1 a) as reasonable biological target for the prevention of treatment (e.g. cancer drugs) related renal toxicity linked to proximal tubular transport processes [35], b) as protein of interest for an improved understanding of the biology of inner ear function and hearing problems, and potentially also c) for a role in male fertility.

Author Contributions

All authors together generated and gathered the patient, animal, genetic and molecular data and analyzed the data. Drs. Robert Kleta, Tzipora C. Falik Zaccai, and Richard Warth vouch for the data and the analysis. All authors helped writing the paper, and all together decided to publish this paper.

Acknowledgements

We are grateful to all of our patients and their families for their kind and significant engagement.

Disclosures

The authors have nothing to disclose.

Funding

DB and RK were supported by the Mitchell Charitable Trust, Kids Kidney Research, Kidney Research UK, the Lowe Syndrome Trust, and the Grocers' Charity. RK was supported by the David and Elaine Potter Charitable Foundation. RK, DB, EDK and HCS were supported by St Peter's Trust for Kidney, Bladder & Prostate Research. DB is supported by the NIHR Biomedical Research Centre at GOSH/ICH. RW was supported by the Deutsche Forschungsgemeinschaft (DFG, German Research Foundation), project number 387509280, SFB 1350. ML and JR were supported by the Lowe Syndrome Trust (MU/ML/2016) and the Erasmus program, respectively. BD and AC-S were supported by the Wellcome Trust [203141/Z/16/Z].

Supplemental Material Table of Contents

(All Supplemental Material is organized in a single pdf-file)

References

1. Conner SD, Schmid SL: Regulated portals of entry into the cell. Nature 422**:** 37-44, 2003 doi: 10.1038/nature01451
2. Christensen EI, Birn H: Megalin and cubilin: multifunctional endocytic receptors. Nat Rev Mol Cell Biol 3**:** 256-266, 2002
3. Kantarci S, Al-Gazali L, Hill RS, Donnai D, Black GC, Bieth E, et al.: Mutations in LRP2, which encodes the multiligand receptor megalin, cause Donnai-Barrow and facio-oculo-acoustico-renal syndromes. Nat Genet 39**:** 957-959, 2007 doi: 10.1038/ng2063
4. Aminoff M, Carter JE, Chadwick RB, Johnson C, Grasbeck R, Abdelaal MA, et al.: Mutations in CUBN, encoding the intrinsic factor-vitamin B12 receptor, cubilin, cause hereditary megaloblastic anaemia 1. Nat Genet 21**:** 309-313, 1999 doi: 10.1038/6831
5. Tanner SM, Aminoff M, Wright FA, Liyanarachchi S, Kuronen M, Saarinen A, et al.: Amnionless, essential for mouse gastrulation, is mutated in recessive hereditary megaloblastic anemia. Nat Genet 33**:** 426-429, 2003 doi: 10.1038/ng1098
6. Eshbach ML, Weisz OA: Receptor-mediated endocytosis in the proximal tubule. Annu Rev Physiol 79**:** 425-448, 2017 doi: 10.1146/annurev-physiol-022516-034234
7. Mintz L, Galperin E, Pasmanik-Chor M, Tulzinsky S, Bromberg Y, Kozak CA, et al.: EHD1 - an EH-domain-containing protein with a specific expression pattern. Genomics 59**:** 66-76, 1999 doi: 10.1006/geno.1999.5800
8. Naslavsky N, Caplan S: EHD proteins: key conductors of endocytic transport. Trends Cell Biol 21**:** 122-131, 2011 doi: 10.1016/j.tcb.2010.10.003
9. Deo R, Kushwah MS, Kamerkar SC, Kadam NY, Dar S, Babu K, et al.: ATP-dependent membrane remodeling links EHD1 functions to endocytic recycling. Nat Commun 9**:** 5187, 2018 doi: 10.1038/s41467-018-07586-z
10. Rainey MA, George M, Ying G, Akakura R, Burgess DJ, Siefker E, et al.: The endocytic recycling regulator EHD1 is essential for spermatogenesis and male fertility in mice. BMC Dev Biol 10**:** 37, 2010 doi: 10.1186/1471-213X-10-37
11. Posey AD, Jr., Swanson KE, Alvarez MG, Krishnan S, Earley JU, Band H, et al.: EHD1 mediates vesicle trafficking required for normal muscle growth and transverse tubule development. Dev Biol 387**:** 179-190, 2014 doi: 10.1016/j.ydbio.2014.01.004
12. Arya P, Rainey MA, Bhattacharyya S, Mohapatra BC, George M, Kuracha MR, et al.: The endocytic recycling regulatory protein EHD1 Is required for ocular lens development. Dev Biol 408**:** 41-55, 2015 doi: 10.1016/j.ydbio.2015.10.005
13. Rapaport D, Auerbach W, Naslavsky N, Pasmanik-Chor M, Galperin E, Fein A, et al.: Recycling to the plasma membrane is delayed in EHD1 knockout mice. Traffic 7**:** 52-60, 2006 doi: 10.1111/j.1600-0854.2005.00359.x
14. Bhattacharyya S, Rainey MA, Arya P, Mohapatra BC, Mushtaq I, Dutta S, et al.: Endocytic recycling protein EHD1 regulates primary cilia morphogenesis and SHH signaling during neural tube development. Sci Rep 6**:** 20727, 2016 doi: 10.1038/srep20727
15. Klootwijk ED, Reichold M, Helip-Wooley A, Tolaymat A, Broeker C, Robinette SL, et al.: Mistargeting of peroxisomal EHHADH and inherited renal Fanconi's syndrome. N Engl J Med 370**:** 129-138, 2014 doi: 10.1056/NEJMoa1307581
16. Mozere M, Tekman M, Kari J, Bockenhauer D, Kleta R, Stanescu H: OVAS: an open-source variant analysis suite with inheritance modelling. BMC Bioinformatics 19**:** 46, 2018 doi: 10.1186/s12859-018-2030-8
17. Skarnes WC, Rosen B, West AP, Koutsourakis M, Bushell W, Iyer V, et al.: A conditional knockout resource for the genome-wide study of mouse gene function. Nature 474**:** 337-342, 2011 doi: 10.1038/nature10163

18. Oltrabella F, Pietka G, Ramirez IB, Mironov A, Starborg T, Drummond IA, et al.: The Lowe syndrome protein OCRL1 is required for endocytosis in the zebrafish pronephric tubule. PLoS Genet 11**:** e1005058, 2015 doi: 10.1371/journal.pgen.1005058
19. Sharma M, Giridharan SS, Rahajeng J, Naslavsky N, Caplan S: MICAL-L1 links EHD1 to tubular recycling endosomes and regulates receptor recycling. Mol Biol Cell 20**:** 5181-5194, 2009 doi: 10.1091/mbc.E09-06-0535
20. Rahajeng J, Giridharan SS, Cai B, Naslavsky N, Caplan S: MICAL-L1 is a tubular endosomal membrane hub that connects Rab35 and Arf6 with Rab8a. Traffic 13**:** 82-93, 2012 doi: 10.1111/j.1600-0854.2011.01294.x
21. Giridharan SS, Cai B, Vitale N, Naslavsky N, Caplan S: Cooperation of MICAL-L1, syndapin2, and phosphatidic acid in tubular recycling endosome biogenesis. Mol Biol Cell 24**:** 1776-1715, 2013
22. Lu Q, Insinna C, Ott C, Stauffer J, Pintado PA, Rahajeng J, et al.: Early steps in primary cilium assembly require EHD1/EHD3-dependent ciliary vesicle formation. Nat Cell Biol 17**:** 228-240, 2015 doi: 10.1038/ncb3109
23. Xie S, Farmer T, Naslavsky N, Caplan S: MICAL-L1 coordinates ciliogenesis by recruiting EHD1 to the primary cilium. J Cell Sci 132, 2019 doi: 10.1242/jcs.233973
24. Sun S, Fisher RL, Bowser SS, Pentecost BT, Sui H: Three-dimensional architecture of epithelial primary cilia. Proc Natl Acad Sci U S A 116**:** 9370-9379, 2019 doi: 10.1073/pnas.1821064116
25. Karczewski KJ, Francioli LC, Tiao G, Cummings BB, Alfoldi J, Wang Q, et al.: The mutational constraint spectrum quantified from variation in 141,456 humans. Nature 581**:** 434-443, 2020 doi: 10.1038/s41586-020-2308-7
26. Lek M, Karczewski KJ, Minikel EV, Samocha KE, Banks E, Fennell T, et al.: Analysis of protein-coding genetic variation in 60,706 humans. Nature 536**:** 285-291, 2016 doi: 10.1038/nature19057
27. Verroust PJ, Birn H, Nielsen R, Kozyraki R, Christensen EI: The tandem endocytic receptors megalin and cubilin are important proteins in renal pathology. Kidney Int 62**:** 745-756, 2002
28. Lee DW, Zhao X, Scarselletta S, Schweinsberg PJ, Eisenberg E, Grant BD, et al.: ATP binding regulates oligomerization and endosome association of RME-1 family proteins. J Biol Chem 280**:** 17213-17220, 2005 doi: 10.1074/jbc.M412751200
29. Naslavsky N, Caplan S: C-terminal EH-domain-containing proteins: consensus for a role in endocytic trafficking, EH? J Cell Sci 118**:** 4093-4101, 2005 doi: 10.1242/jcs.02595
30. Moren B, Shah C, Howes MT, Schieber NL, McMahon HT, Parton RG, et al.: EHD2 regulates caveolar dynamics via ATP-driven targeting and oligomerization. Mol Biol Cell 23**:** 1316-1329, 2012 doi: 10.1091/mbc.E11-09-0787
31. Daumke O, Lundmark R, Vallis Y, Martens S, Butler PJ, McMahon HT: Architectural and mechanistic insights into an EHD ATPase involved in membrane remodelling. Nature 449**:** 923-927, 2007 doi: 10.1038/nature06173
32. Shen J, Scheffer DI, Kwan KY, Corey DP: SHIELD: an integrative gene expression database for inner ear research. Database (Oxford) 2015**:** bav071, 2015 doi: 10.1093/database/bav071
33. Arai M, Mizuta K, Saito A, Hashimoto Y, Iwasaki S, Watanabe T, et al.: Localization of megalin in rat vestibular dark cells and endolymphatic sac epithelial cells. Acta Otolaryngol 128**:** 627-633, 2008 doi: 10.1080/00016480701668531
34. Hosokawa S, Hosokawa K, Ishiyama G, Ishiyama A, Lopez IA: Immunohistochemical localization of megalin and cubilin in the human inner ear. Brain Res 1701**:** 153-160, 2018 doi: 10.1016/j.brainres.2018.09.016
35. Rolleman EJ, Melis M, Valkema R, Boerman OC, Krenning EP, de Jong M: Kidney protection during peptide receptor radionuclide therapy with somatostatin analogues. Eur J Nucl Med Mol Imaging 37**:** 1018-1031, 2010 doi: 10.1007/s00259-009-1282-y

Figures

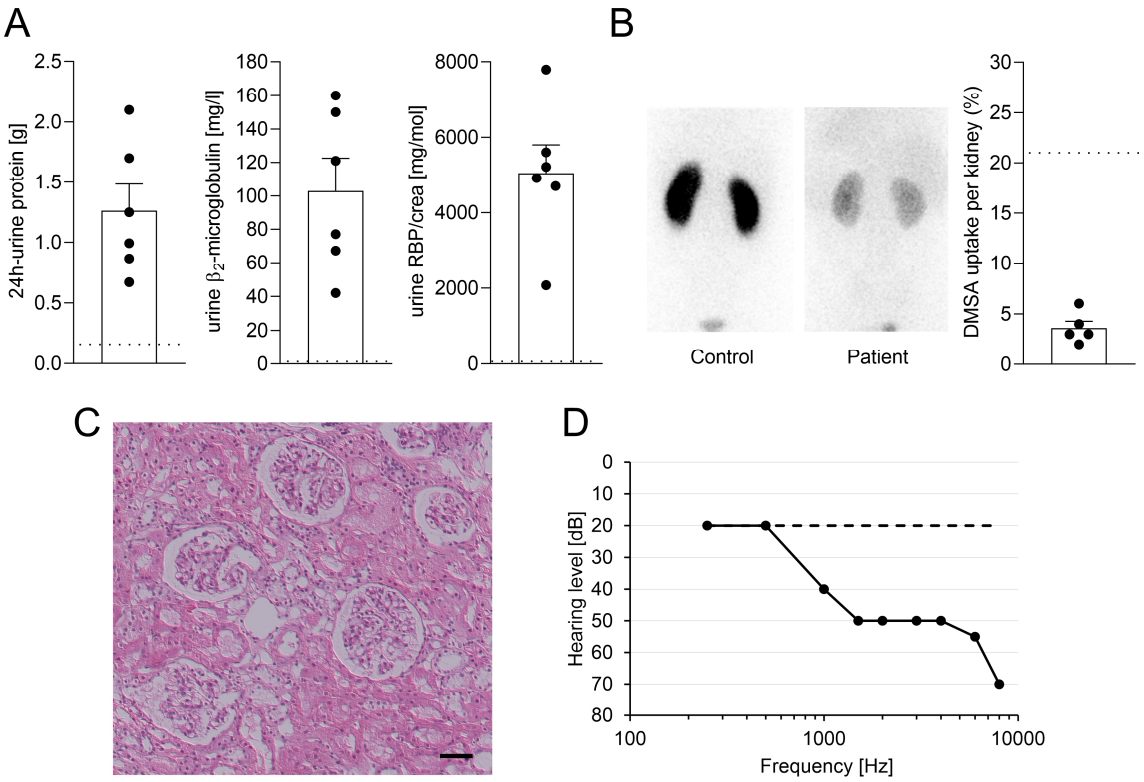

Figure 1: Human phenotype

Shown are key phenotypical features noted in affected individuals. (A) Bar graphs illustrating proteinuria with horizontal dashed black lines indicating the upper limits of normal. 24-h urine protein excretion (left bar) ranges from 0.67 to 2.1 g/d. Proteinuria was predominantly low molecular weight proteinuria as indicated by the highly elevated levels of β_2-microglobulin (middle bar) and retinol binding protein (RBP, normalized to urinary creatinine, right bar). (B) Affected individuals had impaired renal uptake of DMSA. Shown are representative single photon emission tomography (SPECT) images from a healthy control (left panel) and individual 1.1 (right panel) 4 hours after injection of DMSA. Note the markedly decreased global uptake in the affected individual. The bar chart summarizes the results from individuals 1.1, 2.3, 3.1, 3.2, and 4.1.; normal uptake is indicated by the horizontal dashed black line. (C) Patients had normal kidney histology. Shown is a representative image from a kidney biopsy of individual 1.1 stained with hematoxylin and eosin (H&E). Note the normal glomerular, tubular and interstitial morphology (scale bar 50 µm). (D) Affected individuals had sensorineural deafness. Shown is a representative audiogram from affected individual 4.1 (solid line). Note the pronounced hearing loss for higher frequencies compared to control (dashed line).

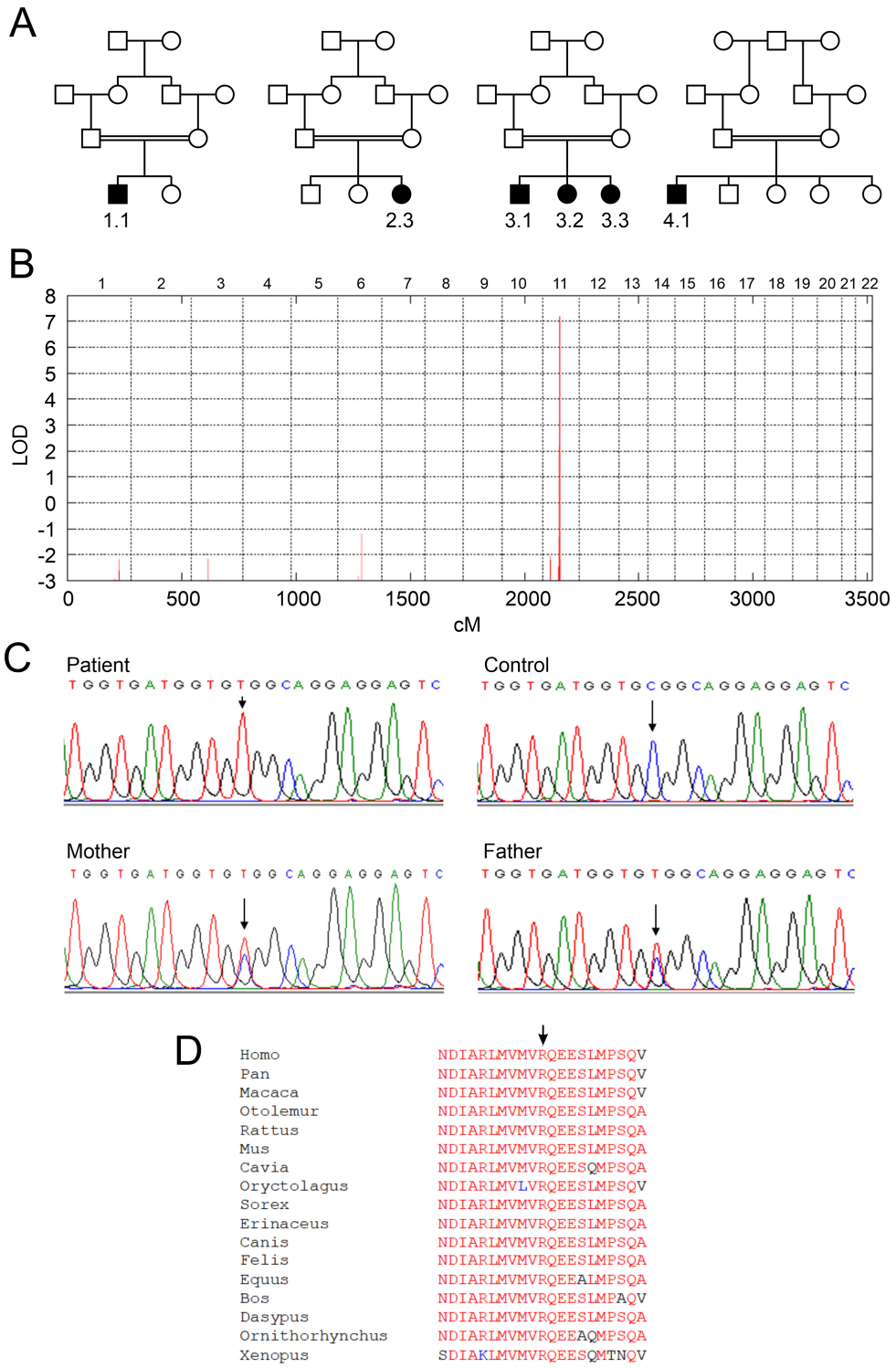

Figure 2: Genetics

(A) Shown are the pedigrees of four families studied suggesting autosomal recessive inheritance. Females are represented by circles and males by squares. A double line between parents indicates consanguinity. Affected individuals are denoted by filled symbols. The numbers below these symbols denote individuals as referred to in the text. (B)The combined multipoint parametric linkage analysis

shows a single genome wide significant peak on chromosome 11, with a maximum LOD score (y-axis) of 7.2. Genetic distance (in centimorgan) and individual chromosomes (1 to 22) are indicated on the lower and upper X-axes, respectively. (C) Representative sequence chromatograms. The EHD1 variant c.1192C>T (indicated by an arrow) is homozygous in an affected individual (left upper panel), absent in the reference sequence (right upper panel) and heterozygous in both parents (lower panels). (D) Regional homology plot of the protein sequence of EHD1 around the change of amino acid 398 from arginine to tryptophan (indicated by arrow). Note the strict and complete evolutionary conservation of R398.

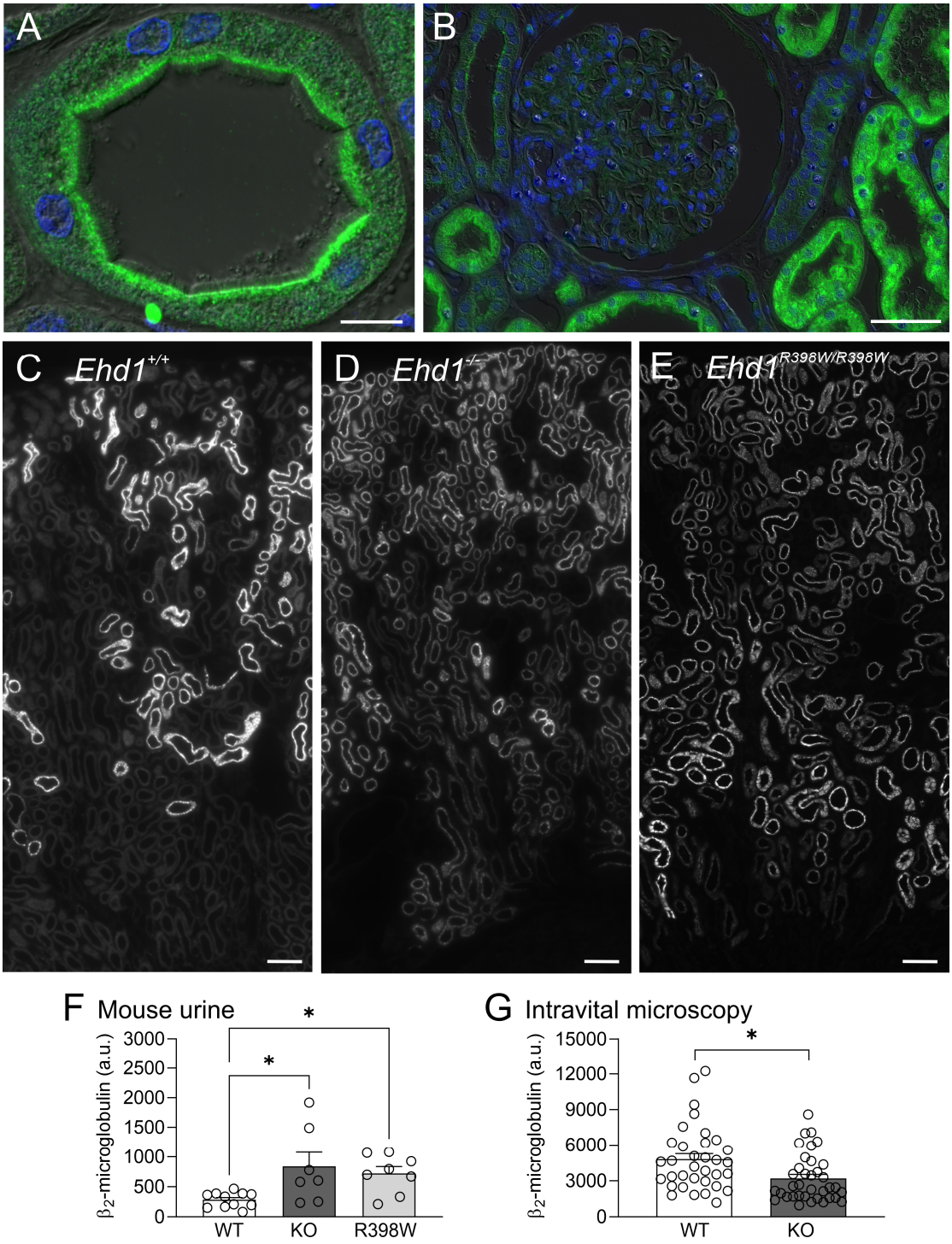

Figure 3: EHD1 localization and function in the kidney

(A) Localization of EHD1 (green) in the normal human proximal tubule. Please note strong EHD1 signal in the subapical compartment beneath the tubular lumen. Nuclear staining (blue); scale bar 10 µm. (B) Normal human kidney showing very little or absent expression of EHD1 (green) within the glomerulus and EHD1 prominence in adjacent proximal tubules. Nuclear staining (blue); scale bar 50

µm. (C-E), Kidney sections showing reabsorption of fluorescently labeled β_2-microglobulin (white) (30 min after injection) in proximal tubules in a wildtype (C), knockout (D) and knockin mouse (E). Note, in wildtype mouse kidney (c) reabsorption of fluorescently labeled β_2-microglobulin was observed mainly in early proximal tubules (S1 and S2 segments). In kidneys of homozygous *Ehd1* knockout (D) or *Ehd1*$^{R398W/R398W}$ mice (E), reabsorption of β_2-microglobulin was not complete after passage of tubular fluid through the early portions of the proximal tubule. Therefore, reabsorption was also observed in late proximal tubules and a spillover of β_2-microglobulin into urine (F) was observed. Scale bars 100 µm. (F) Summary of urinary excretion of labeled β_2-microglobulin during 30 min. Please note the increased urinary loss in homozygous *Ehd1* knockout (KO) and knockin (R398W) mice. Asterisks indicate $p \leq 0.05$ (ANOVA with Dunnett's multiple comparison test). (G) Summary of intravital multiphoton microscopy revealing decreased reabsorption of fluorescently labeled β_2-microglobulin (10 min after injection) into proximal tubules of *Ehd1* knockout mice (symbols indicate individual tubules, 6 animals each group). Asterisk indicates $p \leq 0.05$ (t-test).

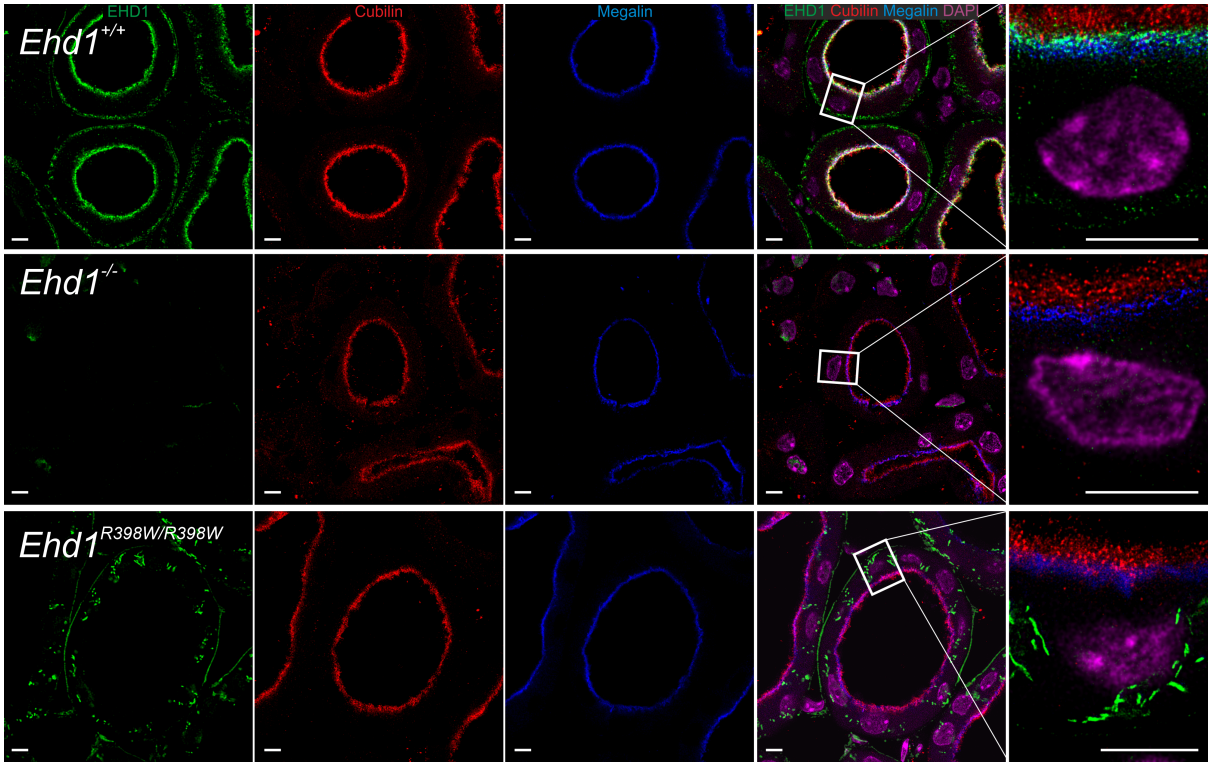

Figure 4: EHD1 localization in relation to Cubilin and Megalin

In wildtype mice (upper row), Ehd1 (green) was predominantly localized in the subapical compartment. Cubilin is shown in red, Megalin in blue, cell nuclei (DAPI) in magenta. In knockout mice (middle row) and knockin mice (lower row), the localization of Cubilin and Megalin appeared unaffected. In knockin mice, Ehd1 abundance was reduced and mutant Ehd1 was observed in intracellular aggregates. Left four panels are confocal images; right high magnification panel: STED image for Ehd1, Cubilin, and Megalin. Deconvolution of all images was performed using Huygens software. Scale bar: 5 µm.

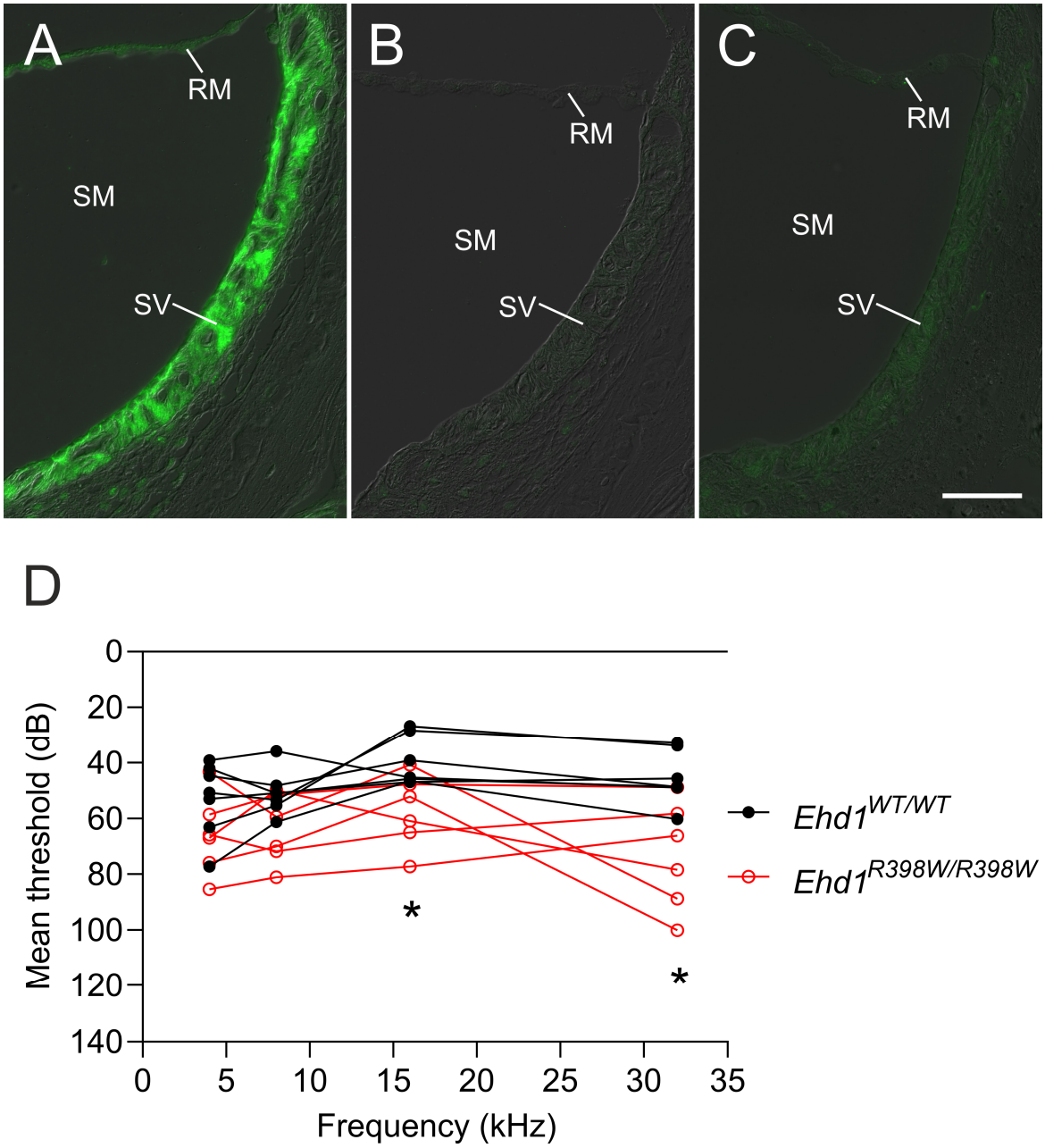

Figure 5: Ehd1 and inner ear

(A) Localization of Ehd1 (green) in stria vascularis (inner ear). In wildtype mice, Ehd1 was strongly expressed in the stria vascularis (SV). In homozygous knockout (B) and knockin mice (C) the labeling of stria vascularis (SV) and Reissner membrane (RM) was absent or grossly diminished, respectively. (SM) scala media (containing endolymph); scale bar 50 µm. (D) Auditory brainstem response measurements of mice revealed a high-frequency hearing impairment in homozygous knockin mice (*Ehd1*$^{R398W/R398W}$, n=6, red symbols) compared to wildtype mice (*Ehd1*$^{wt/wt}$, n=7, black symbols). Please note the reverse scaling of the y-axis to facilitate comparison with the hearing phenotype of the

patient shown in Figure 1. Asterisks indicates $p \leq 0.05$ between groups (t-test with Bonferroni-Dunn correction for multiple testing).

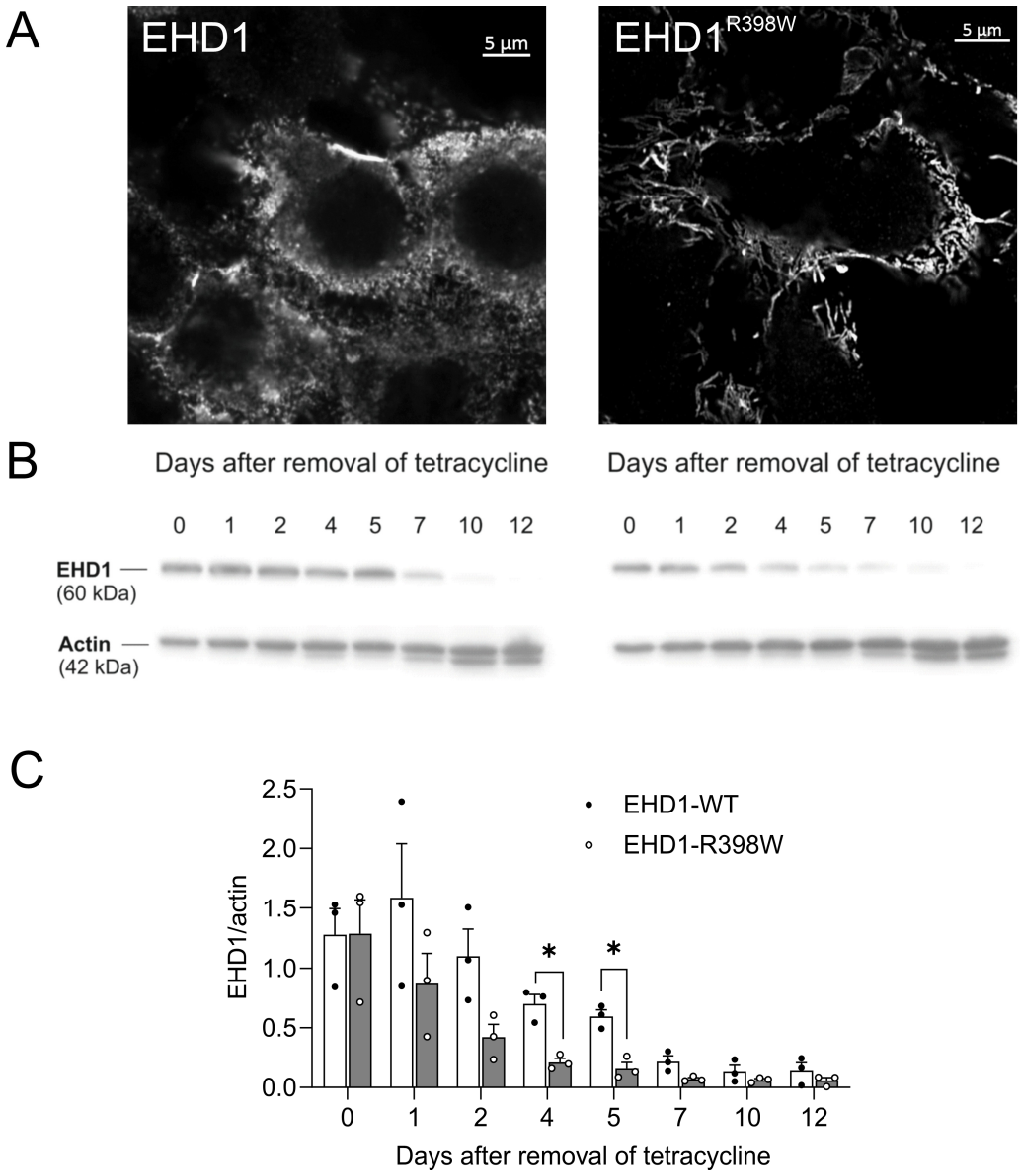

Figure 6: Cellular consequences of mutant EHD1 and protein stability

(A) Immunostained human EHD1 in inducible porcine proximal tubular cells (LLC-PK1). Please note the "spotty" pattern in cells expressing wildtype EHD1 (left panel) and long intracellular structures, presumably tubular recycling endosomes, decorated with $EHD1^{R398W}$. (B)Western blot of cell lysates after removal of tetracycline that was used to induce expression of wildtype or mutant EHD1. Please note the faster decay of EHD1 protein in cells expressing mutant EHD1. (C) Summary of experiments as depicted in (B). EHD1-WT (white bars, filled black symbols), $EHD1^{R398}$ (gray bars, open symbols). Error bars indicate SEM, asterisks $p \leq 0.05$.

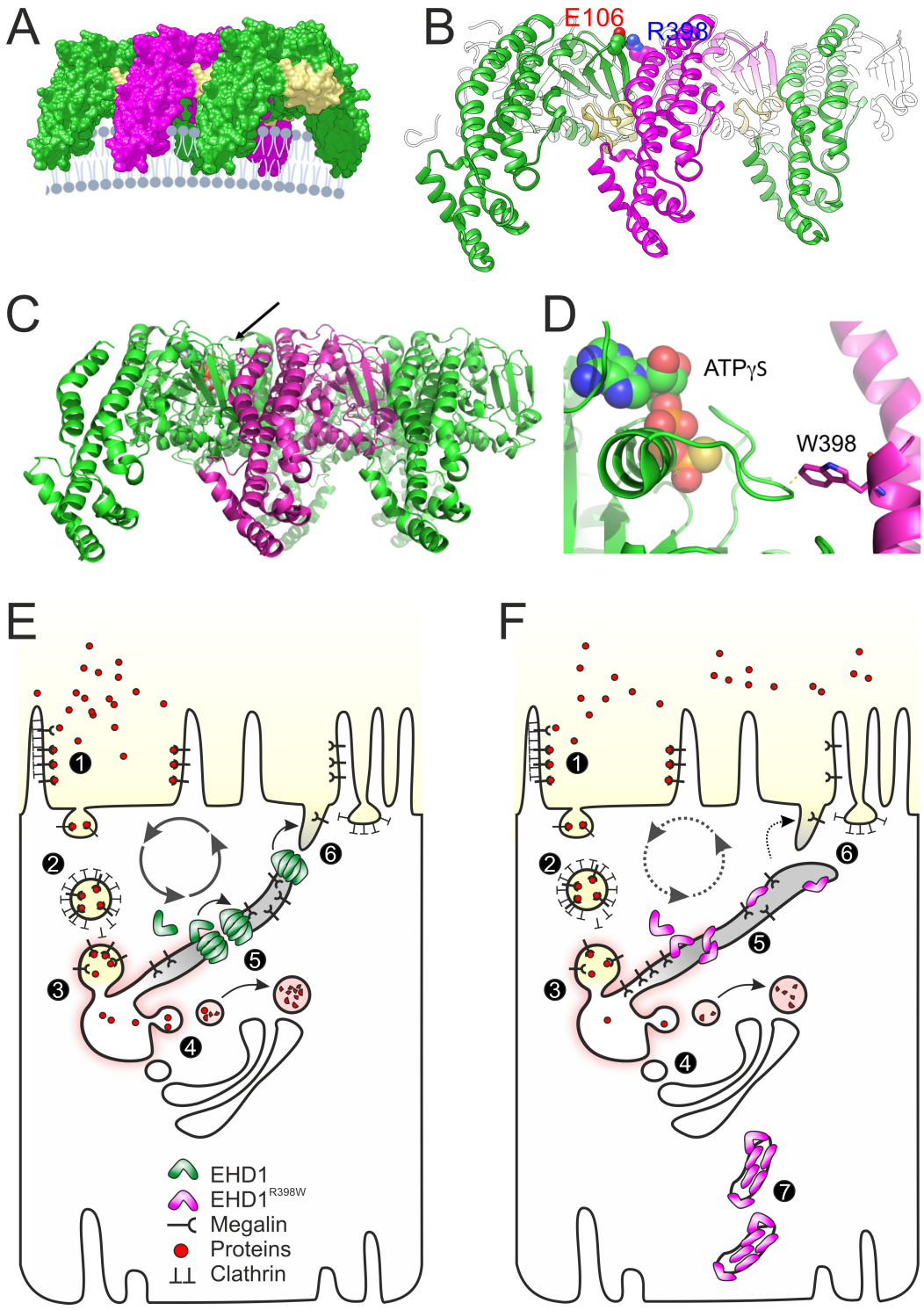

Figure 7: Structural consequences and cell model

(A) Three copies of the activated EHD1 homology model were arranged as oligomer similar to the packing of EHD4 in the crystal (pdb entry code 4CDI). A potential arrangement of the EHD1 oligomer (here trimer of dimers) at the membrane is visualized. The KPF loop (colored in yellow) of one dimer

facilitates major dimer-dimer contacts allowing for a repetitive back-to-front arrangement of EHD1 dimers. (B) Homology modelling suggested that Arg398 located at the tip of α_{12} faces towards the dimer-interface. A possible interaction that would contribute to the dimer-interactions is Glu106-Arg398, which would further stabilize the interaction of the KPF loop (Pro110-Arg135) with α_{12}. (C) Side-on view of oligomeric form of EHD4. Membrane binding is predicted to be at the bottom. The arrow indicates the position of the mutated residue at equivalent position 398 in EHD1. (D) Zoomed view of the tryptophan (W) at the equivalent position 398 in human EHD1. The W is shown in stick representation, projecting close to a loop of the nucleotide-binding pocket. ATPγS is shown bound in this pocket in space filling representation. Note the close proximity of the W residue, which is likely to constrain nucleotide binding, hydrolysis or release by EHD1.

(E) Simplified model of endocytosis and recycling of membranes and receptors in normal proximal tubules. (1) At the base of the brush border membrane, after Megalin and Cubilin (not shown) bind their ligands, such as filtered proteins, the plasma membrane forms invaginations, mostly via Clathrin-coated pits, which lead to the formation of endosomes (2). The endosomes are further processed into sorting endosomes (3) and the endocytic recycling compartment (SE/ERC). Low pH in vacuoles contributes to the separation of ligands from their receptors (4). From the endocytic vacuoles/recycling endosomes, cargo-containing vesicles are directed to multivesicular bodies (not shown) and finally to lysosomes. Receptor-containing vesicles are redirected to the apical membrane (via dense apical tubules). EHD1 and its dimers/oligomers are involved fission of endocytic vesicles (5) and support receptor recycling (6). (F) Vesicle cleavage is impaired in EHD1 patients and knockin mice. Mutant EHD1 dysfunction slows the recycling rate and leads to renal tubular proteinuria, as demonstrated in affected individuals and in animal models. In addition, mutant EHD1 forms aggregates in the cytosol. Megalin and Cubilin are not found in these aggregates, suggesting that EHD1 does not physically interact with these receptor proteins.